AFWAL-TR-88-4002

EMPIRICAL FATIGUE CRACK GROWTH DATA FOR A TENSION LOADED THREADED FASTENER

Russell R. Cervay

University of Dayton Research Institute
300 College Park Avenue
Dayton, Ohio 45469

FEBRUARY 1988

Interim Report for Period February 1985 - March 1987

MATERIALS LABORATORY
AIR FORCE WRIGHT AERONAUTICAL LABORATORIES
AIR FORCE SYSTEMS COMMAND
WRIGHT-PATTERSON AIR FORCE BASE, OHIO 45433-6533

NOTICE

When Government drawings, specifications, or other data ar used for any purpose other than in connection with a definitely Government-related procurement, the United States Government incurs no responsibility or any obligation whatsoever. The fact that the Government may have formulated or in any way supplied the said drawings, specifications, or other data, is not to be regarded by implication, or otherwise in any manner construed, as licensing the holder, or any other person or corporation; or as conveying any rights or permission to manufacture, use, or sell any patented invention that may in any way be related thereto.

This report has been reviewed by the Office of Public Affairs (ASD/PA) and is releasable to the National Technical Information Service (NTIS). At NTIS, it will be available to the general public, including foreign nations.

This report has been reviewed and is approved for publication.

David C Watson

DAVID C. WATSON
Engineering and Design Data
Materials Engineering Branch

Clayton L Harmsworth

CLAYTON L. HARMSWORTH
Technical Manager
Engineering and Design Data
Materials Engineering Branch

FOR THE COMMANDER:

T J Reinhart

T. J. REINHART, Chief
Materials Engineering Branch
Systems Support Division
Materials Laboratory

If your address has changed, if you wish to be removed from our mailing list, or if the addressee is no longer employed by your organization, please notify , Wright-Patterson AFB, OH 45433- to help us maintain a current mailing list.

Copies of this report should not be returned unless return is required by security considerations, contractual obligations, or notice on a specific document.

UNCLASSIFIED

SECURITY CLASSIFICATION OF THIS PAGE

REPORT DOCUMENTATION PAGE

Form Approved OMB No. 0704-0188

1a. REPORT SECURITY CLASSIFICATION: Unclassified	1b. RESTRICTIVE MARKINGS
2a. SECURITY CLASSIFICATION AUTHORITY	3. DISTRIBUTION/AVAILABILITY OF REPORT: Approved for public release; distribution unlimited.
2b. DECLASSIFICATION/DOWNGRADING SCHEDULE	
4. PERFORMING ORGANIZATION REPORT NUMBER(S): UDR-TR-88-27	5. MONITORING ORGANIZATION REPORT NUMBER(S): AFWAL-TR-88-4002
6a. NAME OF PERFORMING ORGANIZATION: University of Dayton Research Institute; 6b. OFFICE SYMBOL (If applicable):	7a. NAME OF MONITORING ORGANIZATION: AFWAL/MLSE
6c. ADDRESS (City, State, and ZIP Code): 300 College Park Avenue, Dayton, OH 45469	7b. ADDRESS (City, State, and ZIP Code): Wright-Patterson Air Force Base, OH 45433-6533
8a. NAME OF FUNDING/SPONSORING ORGANIZATION: Air Force Wright Aeronautical Labs/Materials Lab (AFWAL/MLSE); 8b. OFFICE SYMBOL (If applicable): AFWAL/MLSE	9. PROCUREMENT INSTRUMENT IDENTIFICATION NUMBER: F33615-84-C-5130
8c. ADDRESS (City, State, and ZIP Code): Wright-Patterson Air Force Base, OH 45433-6533	10. SOURCE OF FUNDING NUMBERS: PROGRAM ELEMENT NO. 62102F; PROJECT NO. 2418; TASK NO 241807; WORK UNIT ACCESSION NO. 24180703

11. TITLE (Include Security Classification)

EMPIRICAL FATIGUE CRACK GROWTH DATA FOR A TENSION LOADED THREADED FASTENER

12. PERSONAL AUTHOR(S)

Russell R. Cervay

13a. TYPE OF REPORT	13b. TIME COVERED	14. DATE OF REPORT (Year, Month, Day)	15. PAGE COUNT
Interim	FROM 2/85 TO 3/87	February 1988	49

16. SUPPLEMENTARY NOTATION

17. COSATI CODES			18. SUBJECT TERMS (Continue on reverse if necessary and identify by block number)
FIELD	GROUP	SUB-GROUP	Stress Intensity, Crack Growth, Fastener Fracture Mechanics, Thread

19. ABSTRACT (Continue on reverse if necessary and identify by block number)

This project was undertaken to support the recently formed ASTM task group interested in fracture related problems in threaded fasteners. The purpose of the effort is to provide empirical data that could be used in the development and validation of a standard stress intensity solution for a tension loaded thread containing a surface crack emanating from the thread root. A simulated thread test article containing three circumferential grooves was used, rather than a continuous spiraling thread so that the crack plane would always remain perpendicular to the applied load. The profile of the grooves was identical to a 1-inch 12 UN thread. The simulated thread specimens were used in generating constant amplitude fatigue crack growth rate data for a tension loaded thread containing a surface crack.

(continued on reverse side)

20. DISTRIBUTION/AVAILABILITY OF ABSTRACT	21. ABSTRACT SECURITY CLASSIFICATION
☒ UNCLASSIFIED/UNLIMITED ☐ SAME AS RPT ☐ DTIC USERS	Unclassified

22a. NAME OF RESPONSIBLE INDIVIDUAL	22b. TELEPHONE (Include Area Code)	22c. OFFICE SYMBOL
G.J. Petrak	513-255-5063	AFWAL/MLSA

DD Form 1473, JUN 86 *Previous editions are obsolete.* SECURITY CLASSIFICATION OF THIS PAGE

19. ABSTRACT (Continued)

In addition, a second set of fatigue crack growth rate data was generated using an ASTM compact type, C(T), specimen. This set of data was assumed to accurately characterize the test materials crack growth behavior. The generated thread data was reduced to terms of crack growth rate and stress intensity range using four solutions, found in the reference literature, for similar structural configurations. The C(T) data was subsequently used as a standard of comparison for evaluating how well the four reference solutions, under consideration, characterize the materials mechanical behavior.

PREFACE

This interim report was prepared by the Materials Engineering Branch (AFWAL/MLSE), Systems Support Division, Materials Laboratory, Air Force Wright Aeronautical Laboratories, Wright-Patterson Air Force Base, Ohio, under Project 2418, "Aerospace Structural Materials," Task 241807, "Systems Support," Work Unit 24180703, "Engineering and Design Data."

The work herein was performed during the period February 1985 - March 1987. The authors extend special recognition to Mr. Patrick Ertel of the University of Dayton Research Institute for conducting all of the testing and data reporting. The final report was released November 1987.

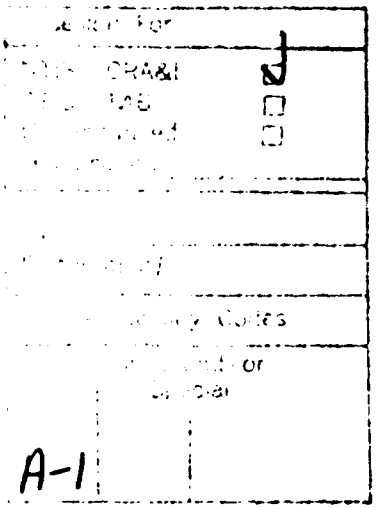

TABLE OF CONTENTS

SECTION		PAGE
I	INTRODUCTION	1
II	MATERIALS, SPECIMENS, AND PROCEDURES	1
III	RESULTS AND DISCUSSION	6
IV	CONCLUSIONS	20
	APPENDIX A	A-1
	APPENDIX B	B-1

LIST OF ILLUSTRATIONS

FIGURE		PAGE
1	Compact-Tension Fatigue Crack Growth Test Specimen	2
2	Simulated Thread Fatigue Crack Growth Test Specimen	3
3	The Thread Root Crack Surface Trace Replica Made by Using Magnetic Rubber Compound	5
4	CT Specimen Fatigue Crack Growth Test Results for 4340 Steel	7
5	Crack Plane Dimensions for Simulated Thread Specimens	8
6	Fracture Face of One of the Simulated Thread Fatigue Crack Growth Rate Specimens	9
7	4340 Steel Fatigue Crack Growth Rate Data, for a Simulated Thread Specimen Loaded in Tension-Tension and Using the Stress Intensity Solution by A.J. Bush	14
8	4340 Steel Fatigue Crack Growth Rate Data, for a Simulated Thread Specimen Loaded in Tension-Tension and Using the Stress Intensity Solution by R.C. Cipolla	15
9	Flaw Shaped Parameter (Q) vs. a/2c for Surface Cracks	17
10	4340 Steel Fatigue Crack Growth Rate Data, for a Simulated Thread Specimen Loaded in Tension-Tension and Using the I.S. Raju and J.C. Newman Stress Intensity Solution	19
11	4340 Steel Fatigue Crack Growth Rate Data, for a Simulated Thread Specimen Loaded in Tension-Tension and Using the Stress Intensity Solution by M. Shiratori	21

LIST OF TABLES

TABLE		PAGE
1	Fracture Face Crack Front Curvature Measurements	10
2	Flow Parameters for Bush Stress Intensity Solution	12
3	Dimensionless Stress Intensity Factor, F_I, for M. Shiratori et. al. Stress Intensity Solution, for a/c = 0.60.	20

I. INTRODUCTION

Recently, ASTM has formed a task group, under Committee E24 on Fracture Testing, to address fracture related problems associated with threaded fasteners. Soon after its inception the task force identified the stress intensity solution for threads as a basic technology needed for application of damage tolerance and durability concepts to fasteners. Some investigators, primarily in the satelite and nuclear industries, have been approximating the stress intensity solution, but none were accepted as accurate. The purpose of this effort was to provide empirical results that could be used in the development and validation of a standardized stress intensity solution for a tension loaded thread containing a surface crack emanating at the thread root. Constant amplitude fatigue crack growth rate tests were performed on specimens with simulated threads. In addition, a set of fatigue crack growth rate data was generated using the standardized C(T) specimen configuration. This second data set was subsequently used as a standard for comparison to the thread data, once the threaded data was reduced in terms of stress intensity factors and crack velocities.

II. MATERIALS, SPECIMEN, AND PROCEDURES

The material selected for this project was 4340 steel heat treated to a hardness of 38 to 39 on the Rockwell "C" scale. The hardness values are equivalent to a tensile strength of 172 to 178 (KSI). A compact type, C(T), specimen was selected for crack growth data generation, the dimensions of which are shown in Figure 1. Three C(T) specimens were made from one-quarter inch thick rolled plate and tested in compliance with ASTM standard E647-86.[1]

The simulated thread specimens were made from 1-inch square bar as shown in Figure 2. The chemical constituent compositions of both wrought products was within specification limits. Microphotographs revealed very similar grain structure for the two material sources. The specimens had three concentric grooves

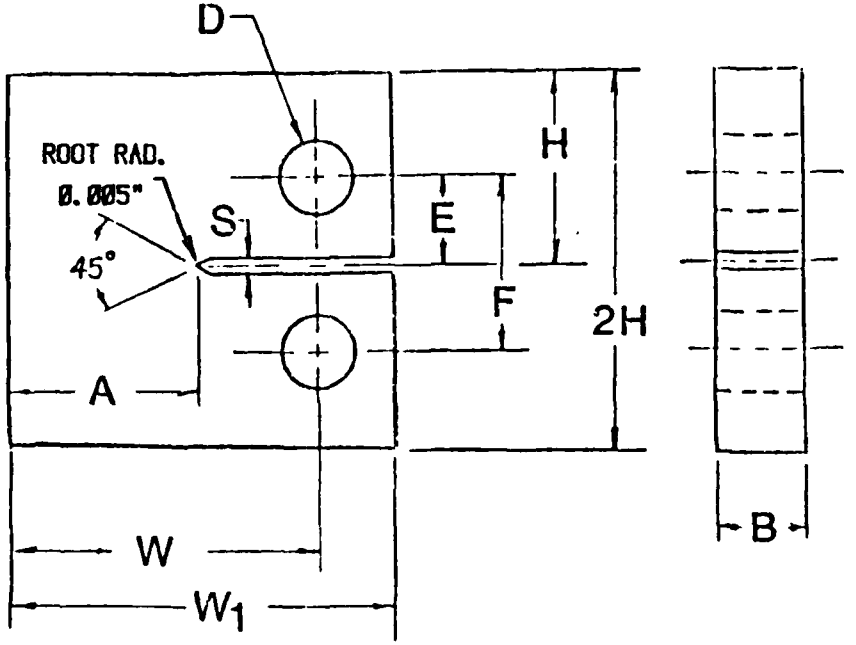

NOTES :

1. All dimensions in inches ± .003
2. Surface finish 32 RMS
3. All surfaces to be ⊥ & // to within .002 TIR

B	A	W	W_1	S	E	F	H	D
.250	1.250	2.000	2.500	.125MAX.	.550	1.100	1.200	.500

CRACK GROWTH SPECIMEN

Figure 1. Compact-tension fatigue crack growth test specimen.

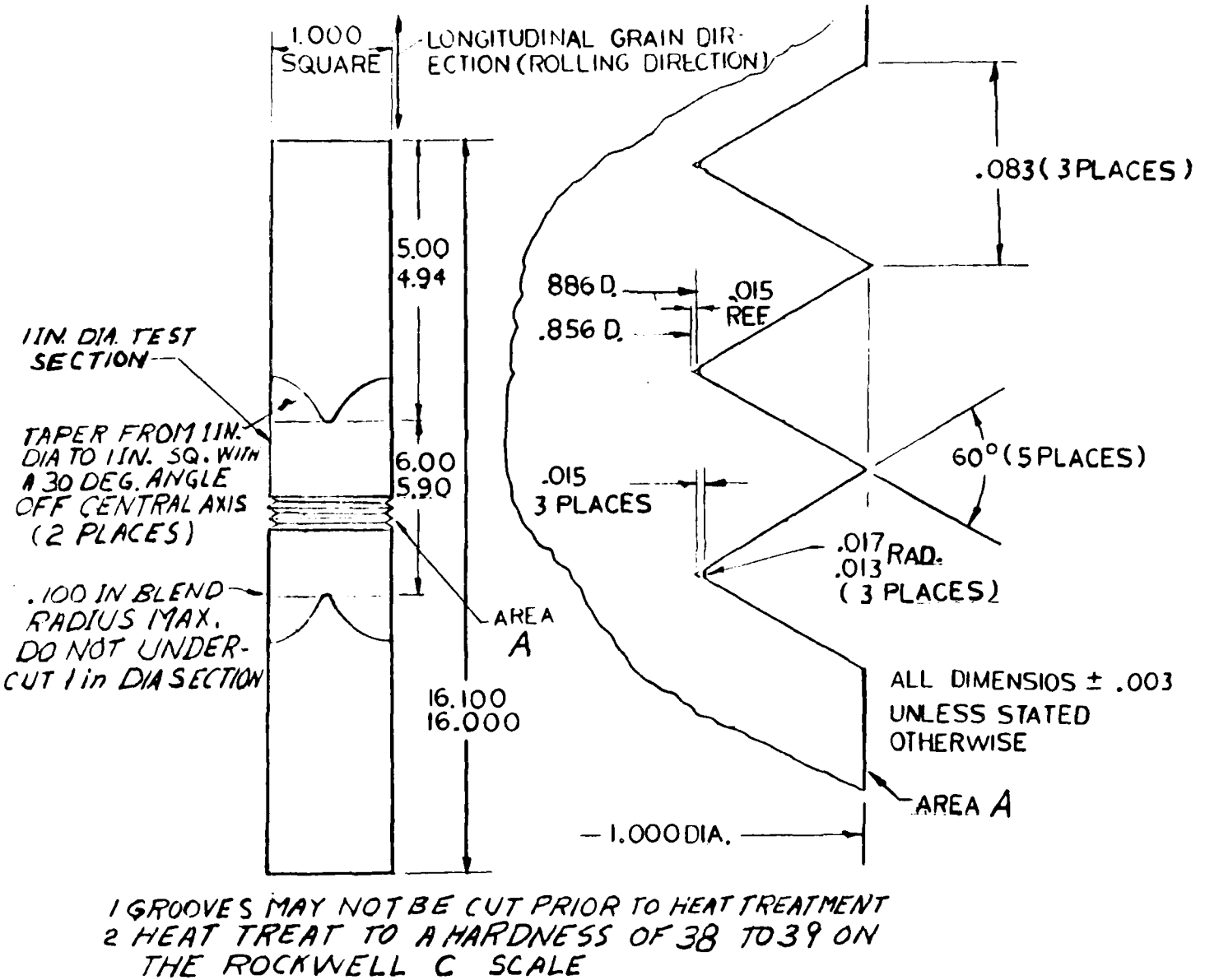

Figure 2. Simulated thread fatigue crack growth test specimen.

rather than a continuous spiraling thread so that cracking was always normal to the applied load. The dimensions of the three grooves were identical to that of a 1-inch 12 UN thread. The two outer grooves were included so as to have the stress distribution at the center groove more closely resemble that of a continuous thread, containing a flaw, remote from the two endmost threads. For the first fatigue test the crack initiated in an outer groove. This problem was overcome in subsequent tests by dimpling the root of the central groove with an electrical discharge welder to create a crack initiation sight. All testing of both specimen configurations were performed under tension-tension loading, in room temperature laboratory air environment and using a load ratio, R, equal to 0.1. A sinusoidal load waveform was used at a frequency of 20 Hz. Periodically, load cycling was interrupted for a crack length measurement. Since it was difficult to visually measure the surface trace at the root of the groove, it became necessary to replicate the crack, using a magnetic-rubber NDI technique, followed by measuring the replicated crack impression with a 20X micrometer thread traveling microscope.

Magnetic rubber is a two-part, thermal setting, polymeric compound containing small iron filings in suspension. Periodically, load cycling was interrupted and a temporary dam was attached to the specimens test section. The dam held the mixed compound while it was setting up. Two magnets, joined by an electrical cable, were attached to the specimen, straddling the test section. The magnets cause the suspended iron filings to migrate through the liquid to the crack. The contrasting color of the filings enhances the visibility of the crack replica. After the compound has solidified, the rubber replica is removed, measured, and load cycling continues until failure occurs. Figure 3 shows a replica of the grooves and crack. The concentration of iron fillings, under 0.645 on the scale, represents the dimple caused by the electrical discharge welding machine.

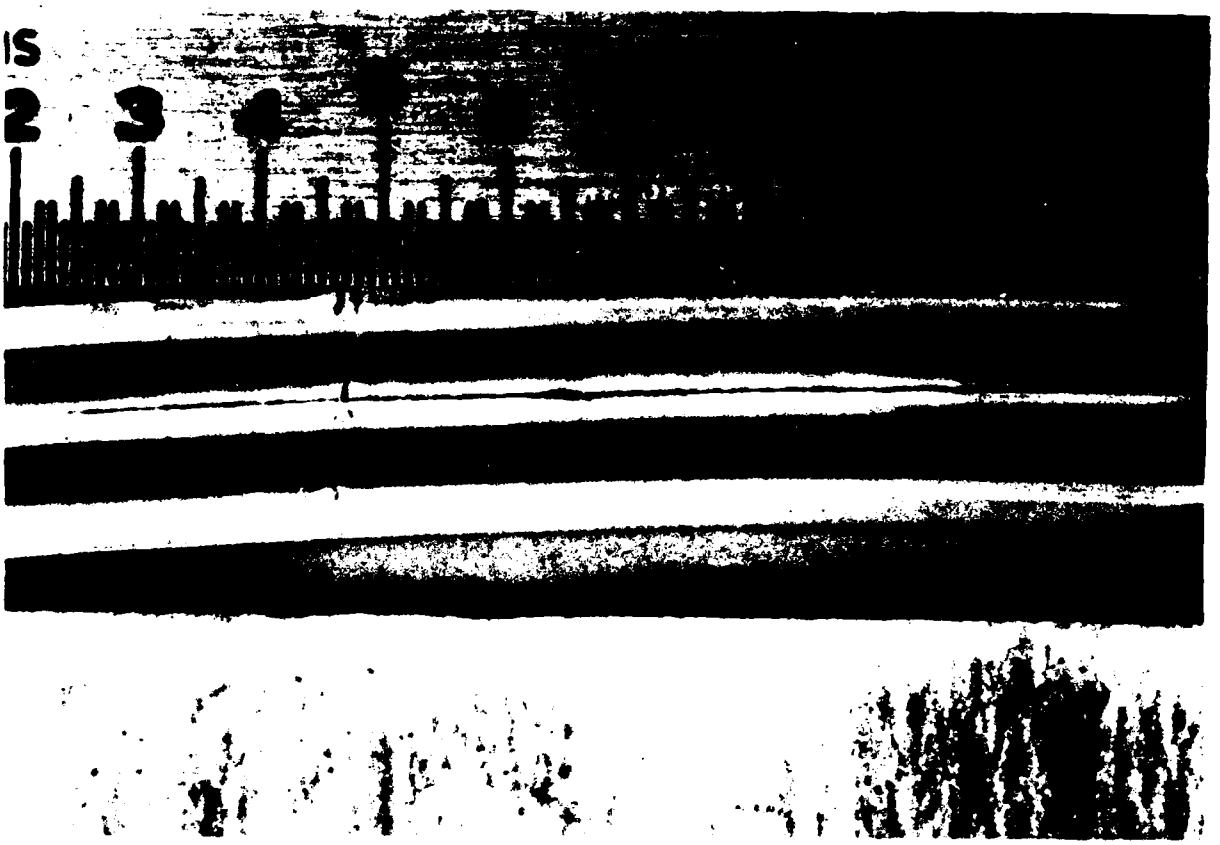

Figure 3. The thread root crack surface trace replica made by using magnetic-rubber compound. The concentration of iron particles, under 0.645 on the scale, represents the dimple caused by the electrical discharge welding machine.

III. RESULTS AND DISCUSSION

The test data for three C(T) specimens, reduced to its final form, is presented in Figure 4. The data plots in a narrow well defined scatter band. As previously mentioned, this data subsequently will serve as a standard of comparison for the simulated thread crack growth data. The C(T) specimen dimensions and test records are presented in Appendix A.

A fifth degree polynomial was fitted to the C(T) data in the following form:

$$\log (da/dn) = 0.858 - 21.575(\log \Delta K_I) + 47.149(\log \Delta K_I)^2 - 39.515(\log \Delta K_I)^3 + 14.821(\log \Delta K_I)^4 - 2.015(\log \Delta K_I)^5 \quad (1)$$

where: ΔK_I = KSI$\sqrt{\text{in.}}$ and,

da/dn = μinch/cycle.

This polynomial representation of the C(T) specimen data was considered, throughout this report, to represent the correct crack growth characteristic for the test material.

The simulated thread crack growth records are included in Appendix B. This data was reduced using four different stress intensity relationships found in the reference literature for structural configurations similar to the fastener situation examined; a plot of the polynomial, equation (1), was subsequently superimposed onto each of the thread data plots, as shown later.

A number of crack length (2c) and corresponding crack depth (a) measurements were taken from clearly marked striations on the round, threaded specimens fracture faces. An illustration of these terms can be seen in Figure 5. A typical fracture face with clearly marked striations is shown in Figure 6. The composite measurements (obtained from eight samples) are listed in Table 1. From these measurements the corresponding thread root surface traces (2s) were calculated. A fourth degree polynomial, equation (2), relating the circumferential surface trace (2s) to the crack depth (a) was fitted to this data:

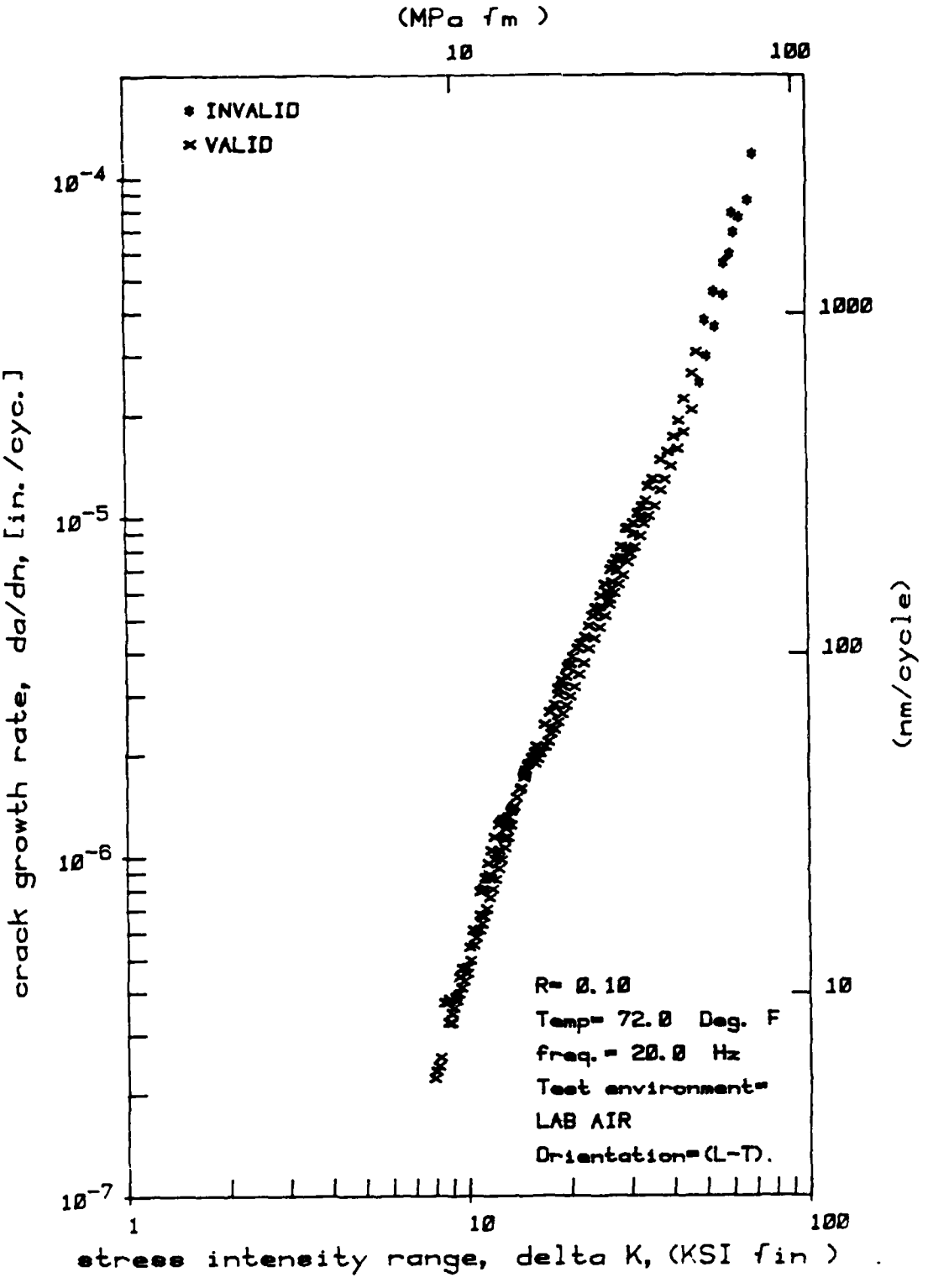

Figure 4. CT specimen fatigue crack growth test results for 4340 steel.

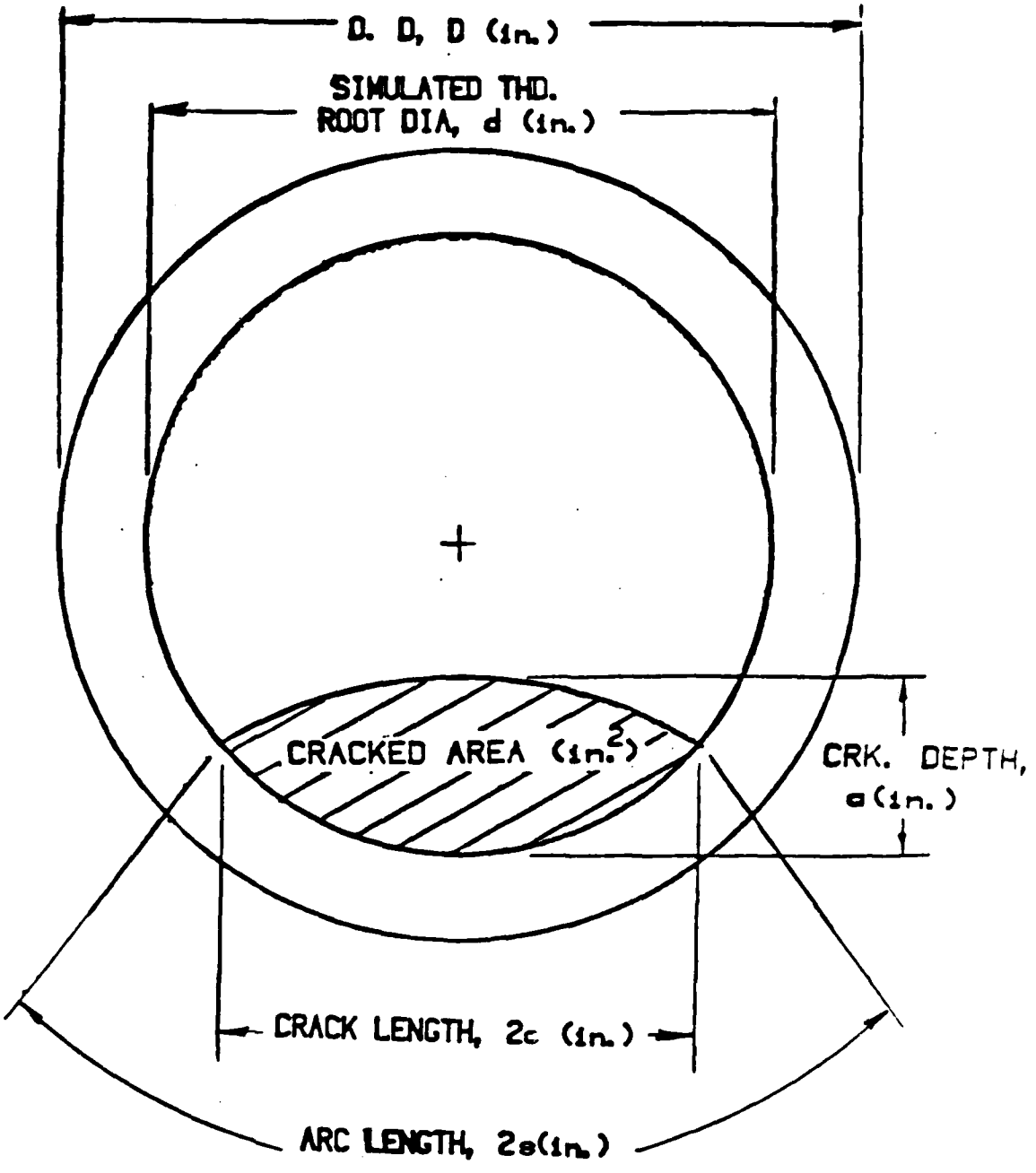

Figure 5. Crack plane dimensions for simulated thread specimens.

Figure 6. Fracture face of one of the simulated thread fatigue crack growth rate specimens.

TABLE 1

FRACTURE FACE CRACK FRONT CURVATURE MEASUREMENTS*

PT NO.	Cord Length 2c(in.)	Arc Length 2s	Depth a(in.)
	depth=a(in.)< minor rad. = $^{d}/_{2}$		
1	0.000	0.000	0.000
2	0.807	1.011	0.314
3	0.573	0.623	0.209
4	0.667	0.754	0.262
5	0.759	0.909	0.289
6	0.837	1.089	0.376
7	0.094	0.094	0.031
8	0.282	0.305	0.103
9	0.729	0.854	0.275
10	0.791	0.974	0.313
11	0.213	0.215	0.075
12	0.466	0.490	0.150
13	0.860	1.166	0.379
14	0.444	0.465	0.150
15	0.682	0.777	0.253
16	0.860	1.166	0.391
17	0.238	0.241	0.072
18	0.619	0.685	0.232
19	0.748	0.888	0.297
	depth = a(in.)>minor rad. = $^{d}/_{2}$		
20	0.904	1.398	0.463
21	0.807	1.785	0.691
22	0.782	1.841	0.694
23	0.813	1.771	0.679
24	0.845	1.682	0.657
25	0.895	1.398	0.445
26	0.801	1.804	0.686
27	0.866	1.605	0.621
28	0.797	1.808	0.676
29	0.826	1.737	0.666
30	0.813	1.771	0.682

* Results of 8 specimens.

$$a\ (in.) = -0.00676 + 0.42402(2s) - 0.24360(2s)^2 + 0.18525(2s)^3 - 0.03394(2s)^4 \quad (2)$$

where: 2s = the thread root surface trace (in.)
a = crack depth (in.)

This polynomial was later used in reducing the round specimens raw data to its final form of crack growth rate, da/dn (in./cycle) versus the stress intensity range, $\Delta K(KSI\sqrt{in.})$.

The first stress intensity solution that was considered was by A.J. Bush.[2] This solution was expected to poorly model a thread because it is for a uniform diameter round bar containing a straight surface crack front, thus it neglects any effect of the crack front curvature and the circumferential grooves. This model takes the form of equation (3).

$$\Delta K_I = Y' \cdot \Delta P/d^{1.5}\ (KSI\sqrt{in.}) \quad (3)$$

where: ΔK_I = stress intensity range $(KSI\sqrt{in.})$
Y' = Bush dimensionless stress intensity factor
ΔP = dynamic load range (KIP)
d = diameter (in.)

The dimensionless stress intensity factor (Y') is a function of the crack depth (a) divided by the diameter (d) which was taken to be the thread root diameter. The root diameter was chosen because for a long thread, remote from the ends, the root diameter is the actual normal load carrying area. Reference 2 presents a table, reproduced here in part as Table 2, for the dimensionless stress intensity factor (Y'). A quadratic function, equation (4), was fitted to the table values.

TABLE 2

FLAW PARAMETERS FOR BUSH* STRESS INTENSITY SOLUTION

Dimensionless Crack Length ($^a/d$)	Dimensionless Stress Intensity Factor Y' **
0.000	0.007
0.050	0.464
0.101	0.762
0.150	1.016
0.201	1.264
0.250	1.491
0.300	1.729
0.334	1.893
0.350	1.977
0.402	2.271
0.449	2.669
0.500	3.348
0.551	4.529
0.602	6.456
0.651	9.515

* Table 2 is from Reference 2 and is reproduced here, in part.

** A quadratic equation was fitted to the table values and subsequently used in calculating the stress intensity using the A.J. Bush solution,

$K_I = Y' \cdot P/d^{1.5}$, where Y' is equal to: $Y' = 0.179 + 0.206(^a/d) + 19.674(^a/d)^2$.

$$Y' = 0.179 + 0.206(a/d) + 19.674(a/d)^2 \quad (4)$$

where: a = crack depth (in.)
d = diameter (in.)

Equation (4) had to be extrapolated beyond the values provided in Table 2 for some of the round specimen data generated here. The round specimens data records were then reduced using equations 2, 3, and 4. The resulting crack growth data is plotted in Figure 7. Repeating, it was anticipated that the Bush solution would underestimate the stress intensity by neglecting: (1) the stress riser associated with the grooves being present, and (2) the crack front curvature. As was expected the calculated crack driving parameter, ΔK, was much lower than what actually existed in the test piece, thus explaining the data points shifted way to the left relative to the line representing the C(T) specimen data.

The second stress intensity solution evaluated was by R.C. Cipolla[3] and takes the form:

$$\Delta K = \Delta Sn/C_k \ (KSI\sqrt{in.}) \quad (5)$$

where: ΔSn = local net stress range (KSI)
C_k = reference flaw factor $(in.)^{-1/2}$

Here the net stress range, ΔSn, is calculated by estimating the remaining load-carrying cross-sectional area. From Reference 3, the reference flaw factor, C_k, equals 2.970 $(1/\mu in.)$ for the thread being modelled. By substituting this value, equation (5) then becomes:

$$\Delta K = \Delta Sn \cdot 0.337 \ (KSI\sqrt{in.}). \quad (6)$$

Test results, for the simulated thread fatigue crack growth data following reduction with equation (6), are presented in Figure 8. The fit to the C(T) data is poor.

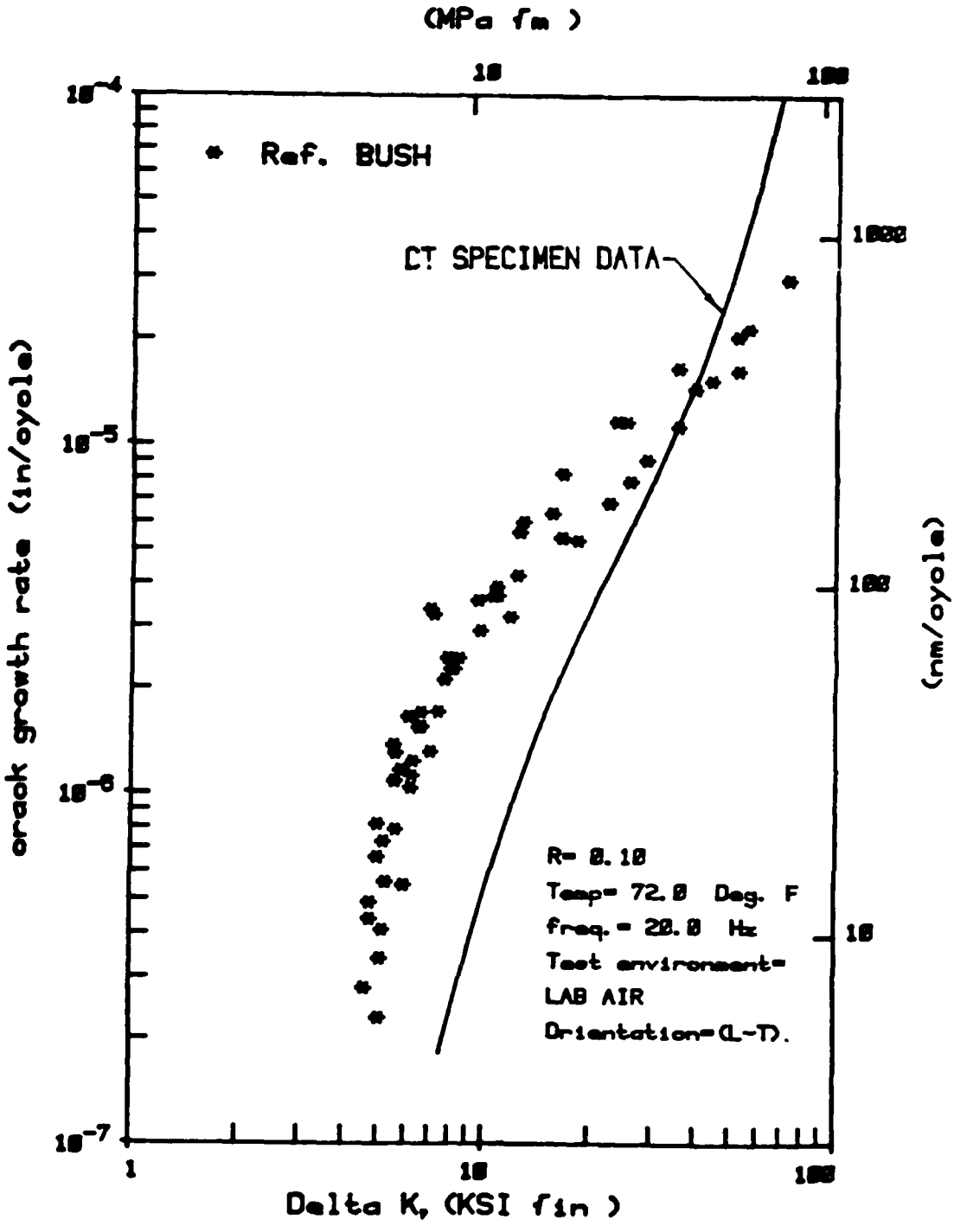

Figure 7. 4340 steel fatigue crack growth rate data, for a simulated thread specimen loaded in tension-tension and using the stress intensity solution by A. J. Bush.

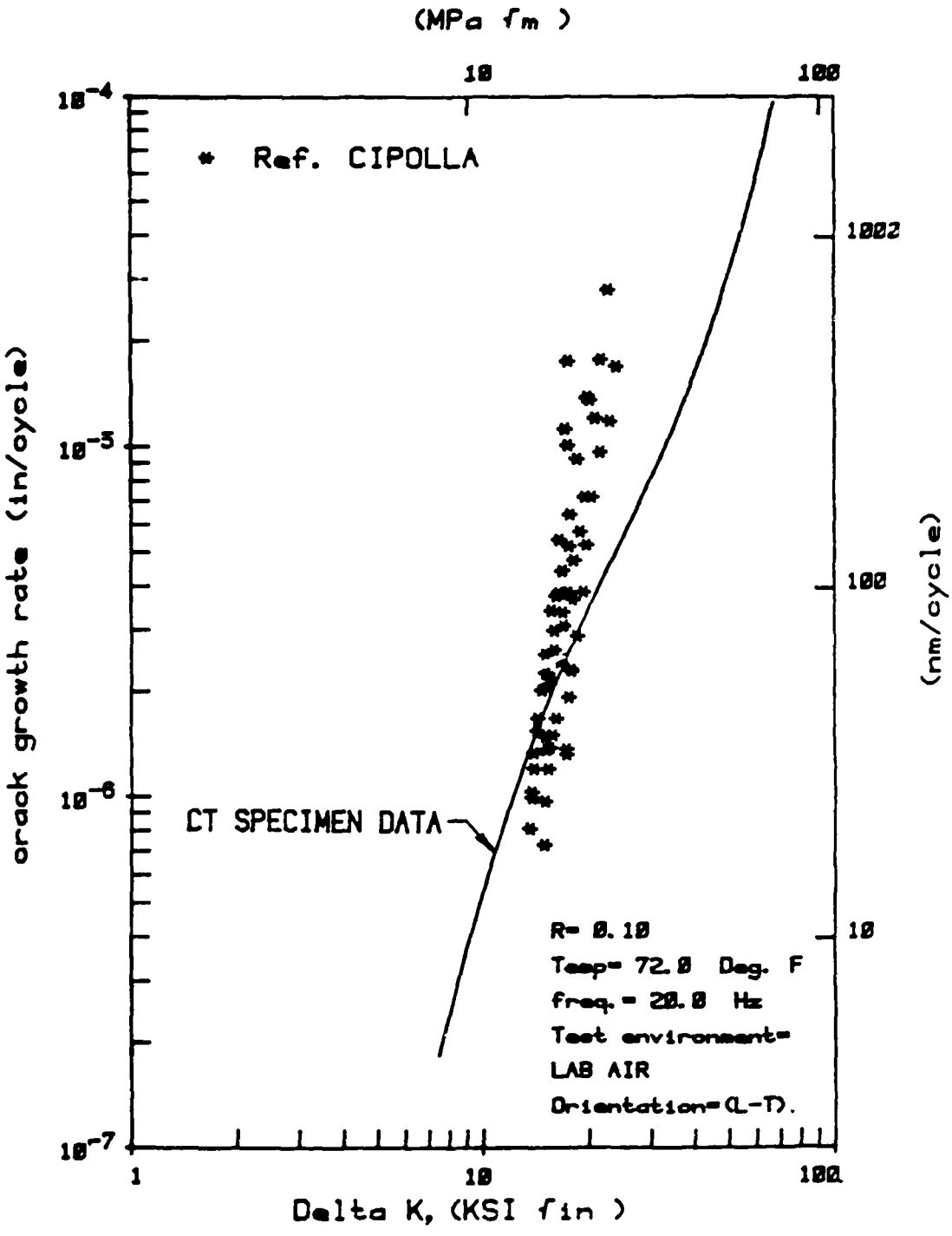

Figure 8. 4340 steel fatigue crack growth rate data, for a simulated thread specimen loaded in tension-tension and using the stress intensity solution by R. C. Cipolla.

The third stress intensity solution used to reduce the crack growth data was by I.S. Raju and J.C. Newman.[4] The solution is for smooth round bar containing a surface crack and takes the form:

$$\Delta K = \Delta Sg \bullet \sqrt{\pi a/Q} \bullet F_A \ (KSI\sqrt{in.}) \qquad (7)$$

where: ΔSg = remote gross tensile stress range (KSI)

Q = elliptical crack shape factor

F_A = boundry correction factor for a surface crack at maximum depth

a = crack depth (in.)

The value for the elliptical crack shape factor, Q, was obtained from Reference 5; the applicable graph is reproduced here as Figure 9. For the developing flaw shape observed in the test articles, and for loading conditions used herein, the elliptical shape factor, Q, is roughly equal to 1.80.

A few values for the boundry correction factor, F_A, at the maximum depth of the curved crack front are presented in Reference 4 as a function (a/d), where "d" is taken to be the specimen's notch diameter, and where (a/c) is the crack depth divided by half the crack length which had to be assumed to remain constant at roughly 0.80. The list of boundry correction factors, F_A, is reproduced here:

a/d	F_A
0.050	1.056
0.125	1.083
0.200	1.131
0.275	1.227
0.350	1.387

A quadratic, equation (8), was fitted to the five values.

$$F_A = 1.0765 - 0.5203 \bullet (a/d) + 3.9873 \bullet (a/d)^2 \qquad (8)$$

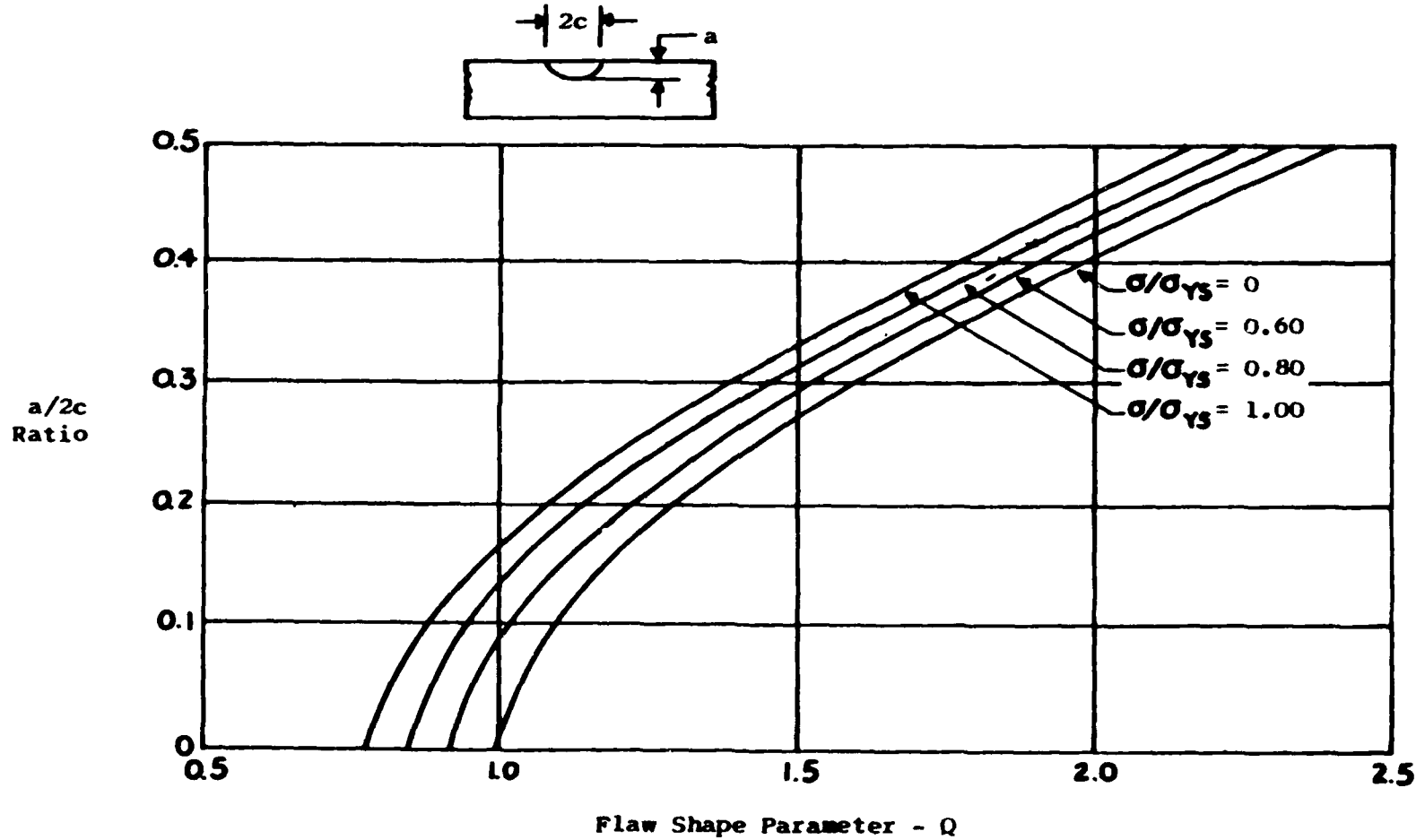

Figure 9. Flaw shaped parameter (Q) vs. $^{a}/2c$ for surface cracks. The figure, from Reference 5, is reproduced here.

Regrettably the actual test data from the simulated thread test articles extends well beyond the maximum (a/d) ratio provided in the reference, thus, necessitating extrapolating equation (8) well beyond the reference values. The remote gross stress range, Sg, was calculated using the remote cross-sectional area, i.e., the area of a 1-inch diameter bar.

Figure 10 presents the reduced data using the Raju and Newman solution. Similar to the A.J. Bush solution the article being modeled is a smooth round tensile loaded bar. As with that solution the reduced round bar specimen data was expected to plot off to the left of the C(T) specimen data, which is not the case. This model predicts the proper trend for the data but is just slightly unconservative, with the data points generally laying below the C(T) results.

The last stress intensity solution to be examined was found in Reference 6, by M. Shiratori, T. Miyoshi, Y. Sakai, and G.R. Zhang. It is for a round bar with a single, central, circumferential groove containing a surface crack. The solution takes the form of equation (9).

$$\Delta K_I = \Delta Sg \cdot \sqrt{\pi \cdot s} \cdot F_I (KSI\sqrt{in.}) \qquad (9)$$

where: ΔK_I = the stress intensity range ($KSI\sqrt{in.}$)

ΔSg = the remote gross tensile stress (KSI)

s = half of the crack tip-to-tip circumferential arc (in.) (see Figure 5)

F_I = Shiratori, et al. dimensionless stress intensity factor at maximum crack depth

A table of values for the dimensionless stress intensity factor, F_I, was found in Reference 6, and is reproduced in part as Table 3. F_I is a function of the depth ratio (a/r), where the flaw aspect ratio (a/c) had to be assumed to remain constant and equal to approximately 0.6. A third-order polynomial, equation (10), was fitted to the tabular data.

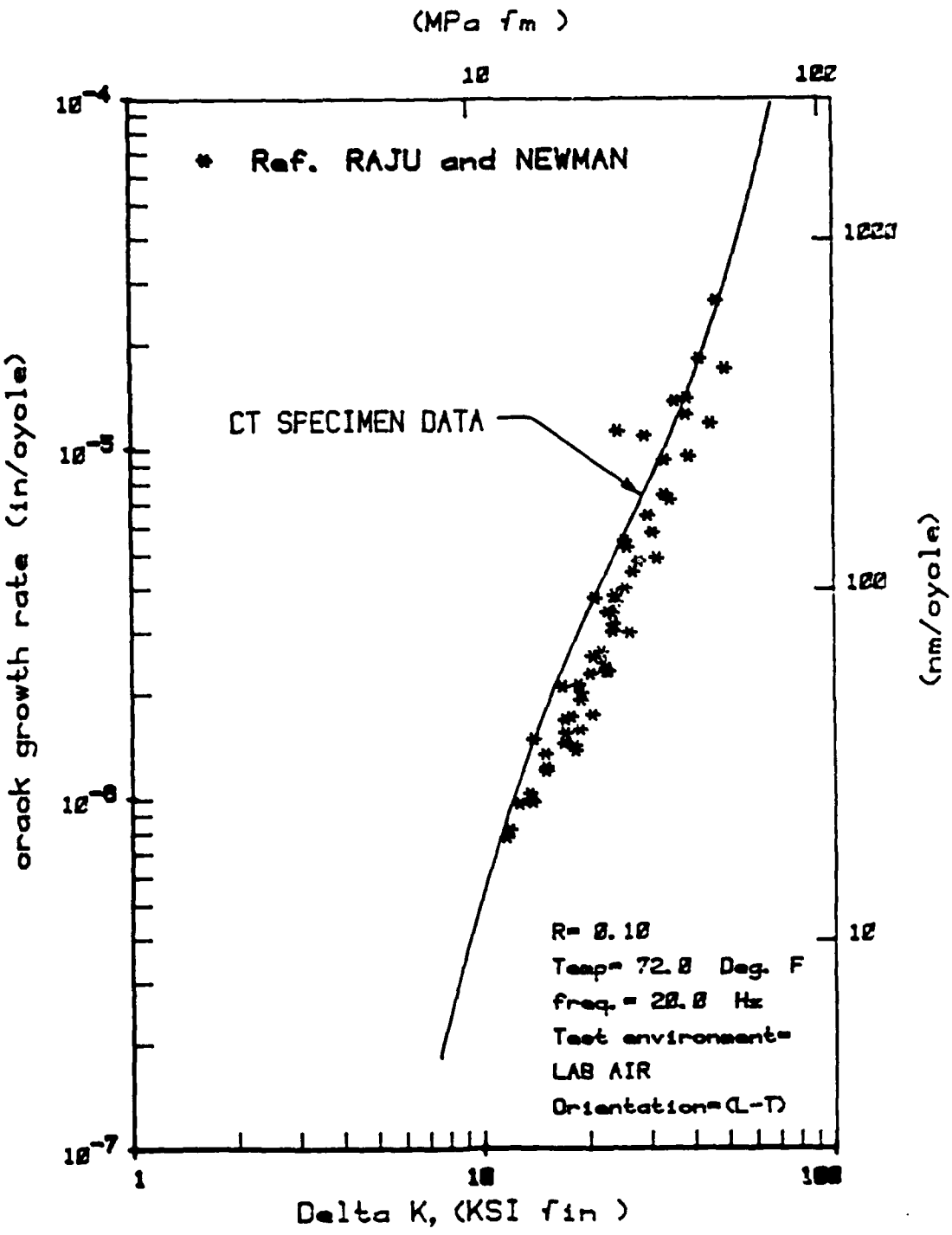

Figure 10. 4340 steel fatigue crack growth rate data, for a simulated thread specimen loaded in tension-tension and using the I. S. Raju and J. C. Newman stress intensity solution.

$$F_I = 0.573 + 0.573(a/r) - 0.857(a/r)^2 + 1.456(a/r)^3 \qquad (10)$$

where: r = major radius equal to approximately 0.5 inch here

For the round specimen test data, the depth ratio (a/r), grew to be considerably greater than the provided data, necessitating extrapolating equation (10) beyond the provided values. The data reduced using equations 9 and 10 is presented in Figure 11. Note that the proper trend is predicted, but is generally conservative, i.e., predicting a slightly faster crack growth rate at a given value of ΔK than that of the C(T) data.

TABLE 3

DIMENSIONLESS STRESS INTENSITY FACTOR, F_I, FOR M. SHIRATORI ET AL. STRESS INTENSITY SOLUTION FOR a/c = 0.60.

Depth Ratio a/r	F_I
0.1	0.525
0.2	0.565
0.4	0.649
0.6	0.840
0.8	1.116
1.0	1.648

IV. CONCLUSIONS

The following conclusions are based on a very limited number of tests. Also, some of the derived functional relationships had to be extrapolated well beyond the reference data used to generate the equations.

1. The A. Bush stress intensity solution poorly modelled the simulated thread fatigue crack growth data as was expected. This can be attributed, in part to: (1) neglecting the crack front curvature and the presence of the groove, and (2) the functional relationship for the dimensionless stress intensity factor had to be extrapolated beyond the values provided in Reference 2.

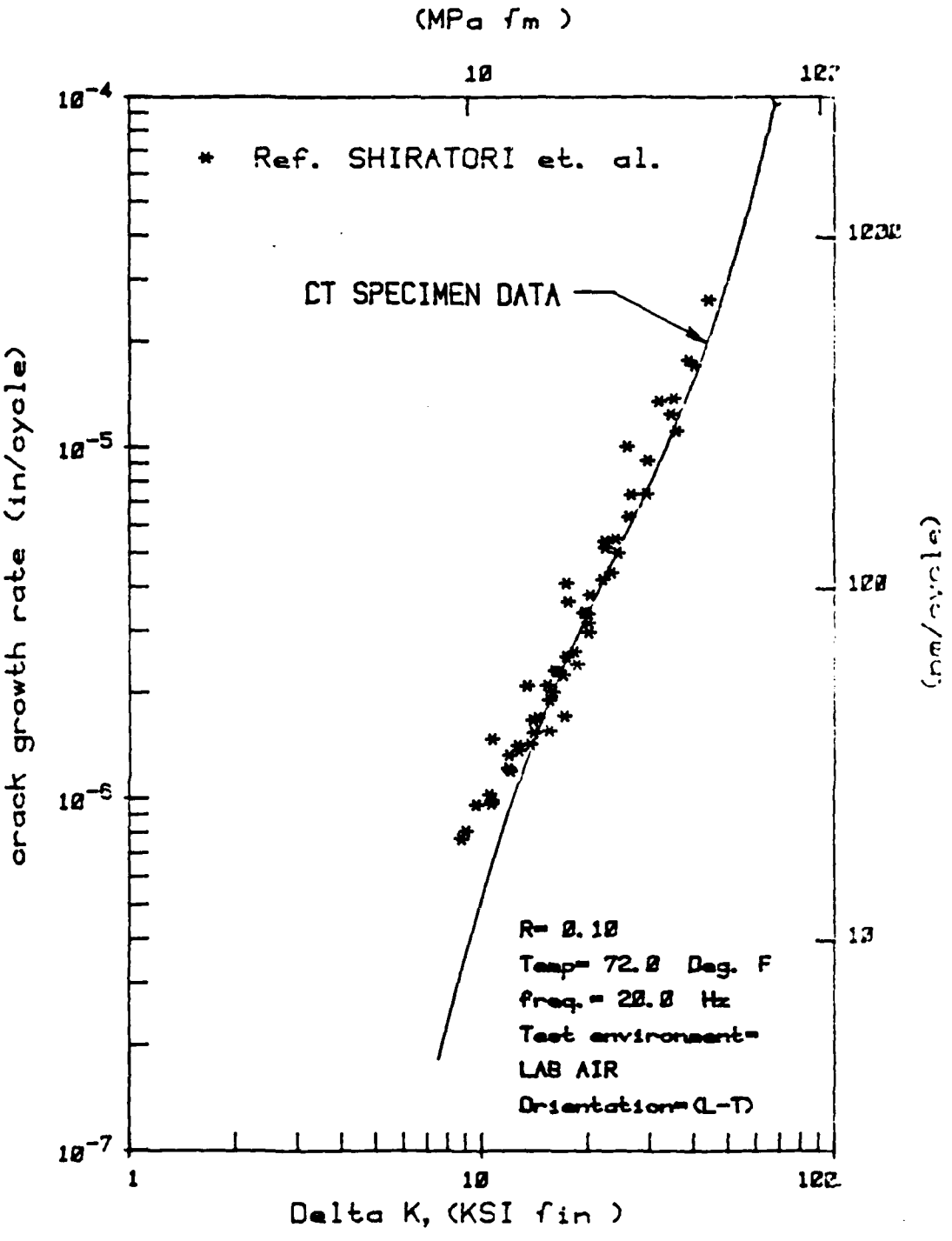

Figure 11. 4340 steel fatigue crack growth rate data, for a simulated thread specimen loaded in tension-tension and using the stress intensity solution by M. Shiratori.

2. The Cipolla stress intensity solution also poorly modelled the thread specimen data which in part could be due to it using the net stress which was difficult to accurately estimate from the cracks circumferential surface trace.

3. The Raju and Newman stress intensity solution models the simulated thread data quite well when you consider it really is for a round bar containing a surface crack. The flaw shape factor, (a/c), had to be assumed to remain a constant in order to use the reference values for the boundary correction factor. Also, the correction factor was estimated by extrapolating the derived function well beyond the values provided in Reference 4.

4. The M. Shiratori solution, which is for a notched bar, approximates the thread data very well in spite of having to extrapolate the equation for the dimensionless stress intensity factor beyond the data provided in Reference 6 and having to assume that the flaw shape factor remained constant throughout the test.

REFERENCES

1. "Constant-Load-Amplitude Fatigue Crack Growth Rate Above 10^{-8} m/cycle," ASTM E-647, 1986.

2. Bush, A.J., "Stress Intensity Factors for Single-Edge-Crack Solid and Hollow Round Bars Loaded in Tension," Journal of Testing and Evaluation, JTEVA, Vol. 9, No. 4, July 1981, pp. 216-223.

3. Cipolla, R.C., "Application of Fracture Mechanics in the Assessment of Threaded Fastener Integrity," Aptech Engineering Services, Inc., Palo Alto, Calif., Paper D7/2.

4. Raju, I.S. and Newman, J.C., NASA Langley Research Center, Hampton, Virginia, presented at Seventeenth National Symposium on Fracture Mechanics, Albany, New York, Aug. 7-9, 1984.

5. Notes from "Third Annual Workshop in Fracture Mechanics," Denver, Colorado, Aug. 7-19, 1966.

6. Shiratori, M., et al., The Society of Mechanics Science, Japan, "Stress Intensity Factors Handbook," Pergamon Press, New York, 1987.

APPENDIX A

COMPACT TENSION SPECIMEN FATIGUE CRACK GROWTH DATA

10-29-86
Specimen No. 3
Pmax = 420 LBF Pmin = 42 LBF R = 0.100
B = 0.249 in. W = 1.990 in. Crack Correction = 0.728 in.

Obs. #	Cycle Count	a-measured
1.000	30.000	0.092
2.000	60.000	0.101
3.000	95.000	0.114
4.000	130.000	0.127
5.000	165.000	0.141
6.000	195.000	0.151
7.000	225.000	0.164
8.000	255.000	0.172
9.000	285.000	0.186
1.000	30.000	0.197
2.000	60.000	0.208
3.000	90.000	0.218
4.000	120.000	0.232
5.000	150.000	0.246
6.000	176.000	0.261
7.000	199.000	0.276
8.000	219.000	0.298
9.000	236.000	0.302
10.000	253.000	0.316
11.000	267.000	0.328
12.000	280.000	0.340
13.000	293.000	0.354
14.000	306.000	0.371
15.000	313.000	0.379
16.000	320.000	0.388
17.000	327.000	0.397
18.000	335.000	0.408
19.000	343.000	0.418
20.000	351.000	0.428
21.000	359.000	0.440
22.000	367.000	0.453
23.000	375.000	0.464
24.000	383.000	0.479
25.000	390.000	0.492
26.000	397.000	0.506
27.000	403.500	0.521
28.000	409.500	0.534
29.000	415.500	0.549
30.000	420.500	0.563
31.000	424.500	0.574
32.000	428.500	0.587
33.000	432.500	0.598
34.000	436.500	0.613
35.000	440.200	0.627
36.000	443.000	0.638

10-29-86
Specimen No. 3 (Continued)
Pmax = 420 LBF Pmin = 42 LBF R = 0.100
B = 0.249 in. W = 1.990 in. Crack Correction = 0.728 in.

Obs. #	Cycle Count	a-measured
1.000	3.000	0.651
2.000	5.800	0.665
3.000	7.600	0.673
4.000	9.300	0.682
5.000	10.800	0.690
6.000	12.400	0.698
7.000	14.000	0.707
8.000	15.500	0.717
9.000	17.100	0.727
10.000	18.700	0.738
11.000	20.300	0.751
12.000	21.900	0.764
13.000	23.300	0.778
14.000	24.700	0.789
15.000	25.900	0.804
16.000	27.000	0.819
17.000	27.900	0.832
18.000	28.500	0.844
19.000	29.100	0.853
20.000	29.700	0.861
21.000	30.200	0.876
22.000	30.460	0.883
23.000	30.960	0.897
24.000	31.310	0.910
25.000	31.560	0.925
26.000	31.820	0.937
27.000	32.050	0.952
28.000	32.270	0.973
29.000	32.360	1.000

11-3-86
Specimen No. 4340-4
Pmax = 400 LBF Pmin = 40 LBF R = 0.100
B = 0.249 in. W = 1.988 in. Crack Correction = 0.730 in.

Obs. #	Cycle Count	a-measured
1.000	67.000	0.084
2.000	108.000	0.091
3.000	158.000	0.102
4.000	190.000	0.110
5.000	231.000	0.118
6.000	281.000	0.130
7.000	321.000	0.140
8.000	361.000	0.151
9.000	401.000	0.161
10.000	441.000	0.174
1.000	30.000	0.184
2.000	65.000	0.194
3.000	95.000	0.204
4.000	125.000	0.215
5.000	155.000	0.228
6.000	185.000	0.240
7.000	215.000	0.252
8.000	245.000	0.265
9.000	275.000	0.278
10.000	305.000	0.294
11.000	323.000	0.304
12.000	343.000	0.316
13.000	360.000	0.327
14.000	377.000	0.337
15.000	394.000	0.349
16.000	411.000	0.360
17.000	426.000	0.372
18.000	440.000	0.384
19.000	453.000	0.396
20.000	465.000	0.406
21.000	477.000	0.418
22.000	487.000	0.430
23.000	497.000	0.440
24.000	507.000	0.453
25.000	516.000	0.466
26.000	524.000	0.478

11-3-86
Specimen No. 4340-4 (Continued)
Pmax = 400 LBF Pmin = 40 LBF R = 0.100
B = 0.249 in. W = 1.988 in. Crack Correction = 0.730 in.

Obs. #	Cycle Count	a-measured
1.000	8.000	0.489
2.000	15.500	0.502
3.000	22.000	0.514
4.000	27.500	0.523
5.000	32.500	0.533
6.000	37.300	0.542
7.000	42.000	0.553
8.000	46.600	0.562
9.000	51.100	0.572
10.000	55.500	0.582
11.000	59.800	0.592
12.000	64.000	0.604
13.000	68.100	0.613
14.000	72.100	0.625
15.000	76.000	0.637
16.000	79.800	0.649
17.000	83.300	0.662
18.000	86.600	0.674
19.000	89.700	0.687
20.000	92.600	0.700
21.000	95.200	0.714
22.000	97.400	0.723
23.000	99.300	0.734
24.000	100.900	0.744
25.000	102.300	0.753
26.000	103.600	0.763
27.000	104.800	0.770
28.000	105.900	0.779
29.000	107.000	0.790
30.000	108.000	0.798
31.000	109.000	0.806
32.000	110.000	0.818
33.000	110.900	0.828
34.000	111.700	0.836
35.000	112.500	0.847
36.000	113.300	0.860
37.000	114.000	0.870
38.000	114.700	0.883
39.000	115.300	0.896
40.600	115.800	0.907
41.000	116.200	0.920
42.000	116.500	0.931
43.000	116.700	0.940
44.000	116.800	0.946
45.000	116.900	0.953
46.000	117.000	0.964

11-3-86
Specimen No. 4340-4 (Continued)
Pmax = 400 LBF Pmin = 40 LBF R = 0.100
B = 0.249 in. W = 1.988 in. Crack Correction = 0.730 in.

Obs. #	Cycle Count	a-measured
47.000	117.100	0.970
48.000	117.200	0.980
49.000	117.300	0.990
50.000	117.400	1.024

11-21-85
Specimen No. 4340-5
Pmax = 460 LBF Pmin = 46 LBF R = 0.100
B = 0.253 in. W = 1.997 in. Crack Correction = 0.717 in.

Obs. #	Cycle Count	a-measured
1.000	30.000	0.071
2.000	70.000	0.082
3.000	110.000	0.094
4.000	150.000	0.106
5.000	190.000	0.120
6.000	205.000	0.125
7.000	228.000	0.133
8.000	266.000	0.144
9.000	304.000	0.163
10.000	330.000	0.174
11.000	352.000	0.184
12.000	373.000	0.196
13.000	393.000	0.205
1.000	44.000	0.217
2.000	60.600	0.228
3.000	91.300	0.240
4.000	115.600	0.261
5.000	123.400	0.278
6.000	155.000	0.298
7.000	163.200	0.304
8.000	169.100	0.309
9.000	185.600	0.327
10.000	197.900	0.337
11.000	205.400	0.344
12.000	223.000	0.365
13.000	231.400	0.372
14.000	236.300	0.379
15.000	251.400	0.398
16.000	258.700	0.410
17.000	262.800	0.415
18.000	271.700	0.428
19.000	282.000	0.445
20.000	285.300	0.451
21.000	290.300	0.460
22.000	299.600	0.479
23.000	303.500	0.486
24.000	309.100	0.498
25.000	314.200	0.509
26.000	317.900	0.519

12-5-86
Specimen No. 4340-5 (Continued)
Pmax = 460 LBF Pmin = 46 LBF R = 0.100
B = 0.253 in. W = 1.997 in. Crack Correction = 0.717 in.

Obs. #	Cycle Count	a-measured
1.000	2.500	0.525
2.000	8.200	0.540
3.000	12.100	0.550
4.000	14.800	0.559
5.000	18.000	0.571
6.000	24.000	0.588
7.000	25.300	0.595
8.000	27.700	0.604
9.000	30.800	0.616
10.000	32.800	0.624
11.000	35.200	0.635
12.000	38.000	0.646
13.000	40.100	0.658
14.000	41.900	0.666
15.000	44.100	0.679
16.000	46.000	0.690
17.000	48.200	0.704
18.000	49.200	0.711
19.000	50.200	0.719
20.000	51.600	0.730
21.000	53.200	0.742
22.000	53.900	0.748
23.000	54.600	0.757
24.000	55.600	0.767
25.000	56.700	0.776
26.000	57.900	0.789
27.000	58.700	0.799
28.000	59.500	0.810
29.000	60.300	0.825

APPENDIX B

SIMULATED THREAD SPECIMEN FATIGUE CRACK GROWTH DATA*

* "CRACK LENGTH" listed in the fourth column equals 2s, or the circumferential surface trace of the crack at the root of the central groove.

Specimen #2A Dia. 0.8890 Area 0.6207 Material 4340 St.

Initial Stress	R-ratio	Initial Loads
55 KSI	0.1	34,139
40 KSI		18,777
		3,414

Insp.	Max. Load	Cycles	Crack Length	Total Cycles
1	34,139	50,900	0.1090	50,900
2	24,828	40,000	0.1349	90,900
3	24,828	21,000	0.2594	111,900
4	24,828	20,000	0.3273	131,900
5	24,828	10,000	0.3952	141,900
6	24,828	10,000	0.4620	151,900
7	24,828	10,000	0.5062	161,900
8	24,828	10,000	0.5804	171,900
9	24,828	10,000	0.7021	181,900
10	24,828	10,000	0.8500	191,900
11	24,828	10,000	1.1042	201,900
12	24,828	8,300	Failure	210,200

Specimen #3A Dia. 0.8896 Area 0.6217 Material 4340 St.

Initial Stress	R-ratio	Initial Loads
48 KSI	0.1	29,842 16,413 2,984

Insp.	Max. Load	Cycles	Crack Length	Total Cycles
1	29,842	80,000	0.1211	80,000
2	29,842	10,000	0.1550	90,000
3	29,842	10,000	0.1650	100,000
4	29,842	10,000	0.2120	110,000
5	29,842	10,000	0.3100	120,000
6	29,842	10,000	0.3152	130,000
7	29,842	10,000	0.3603	140,000
8	29,842	10,000	0.4343	150,000
9	29,842	10,000	0.6404	160,000
10	29,842	10,000	0.7729	170,000
11	29,842	10,000	1.1200	180,000
12	29,842	5,200	Failure	185,200

Specimen #5A Dia. 0.8910 Area 0.6235 Material 4340 St.

Initial Stress	R-ratio	Initial Loads
42 KSI	0.1	26,187 14,403 2,619

Insp.	Max. Load	Cycles	Crack Length	Total Cycles
1	26,187	62,500	0.0563	62,500
2	26,187	17,500	0.1175	80,000
3	26,187	20,000	0.1621	100,000
4	26,187	2,000	0.1984	120,000
5	26,187	2,000	0.2892	140,000
6	26,187	2,000	0.4324	160,000
7	26,187	10,000	0.5563	170,000
8	26,187	5,000	0.6251	175,000
9	26,187	5,000	0.8136	180,000
10	26,187	5,000	1.5085	185,000
11	26,187	5,000	1.5829	190,000
12	26,187	5,000	1.4500+	195,000
13	26,187	5,000	1.1929+	200,000
14	26,187	5,000	1.919	205,000
			Failure	207,700

+ questionable circumferential crack length measurement attributed to poor quality magnetic-rubber replica.

Specimen #6A Dia. 0.8886 Area 0.6202 Material 4340 St.

Initial Stress	R-ratio	Initial Loads
48 KSI	0.1	29,770 16,373 2,977

Insp.	Max. Load	Cycles	Crack Length	Total Cycles
1	29,770	50,000	0.0708	50,000
2	29,770	10,000	0.0863	60,000
3	29,770	20,000	0.1115	80,000
4	29,770	20,000	0.2020	100,000
5	29,770	10,000	0.2110	110,000
6	29,770	10,000	0.2639	120,000
7	29,770	10,000	0.2742	130,000
8	29,770	10,000	0.3270	140,000
9	29,770	10,000	0.4232	150,000
10	29,770	10,000	0.5286	160,000
11	29,770	5,000	0.5704	165,000
12	29,770	5,000	0.6465	170,000
13	29,770	5,000	0.7590	175,000
14	29,770	2,500	0.8829	177,500
15	29,770	2,500	0.9646	180,000
16	29,770	2,500	1.0308	182,500
17	29,770	2,500	1.1725	185,000
18	29,770	2,500	1.4185+	187,500
		1,600	Failure	189,100

Specimen #7A Dia. 0.8917 Area 0.6245 Material 4340 St.

Initial Stress	R-ratio	Initial Loads
38 KSI	0.1	23,731 13,052 2,373

Insp.	Max. Load	Cycles	Crack Length	Total Cycles
1	23,731	100,000	0.0904	100,000
2	23,731	30,000	0.1351	130,000
3	23,731	20,000	0.1646	150,000
4	23,731	20,000	0.2339	170,000
5	23,731	20,000	0.2817	190,000
6	23,731	20,000	0.3615	210,000
7	23,731	15,000	0.4403	225,000
8	23,731	10,000	0.4999	235,000
9	23,731	10,000	0.5888	245,000
10	23,731	10,000	0.6927	255,000
11	23,731	7,500	0.8065	262,500
12	23,731	7,500	0.9585	270,000
13	23,731	7,500	1.2338	277,500
14	23,731	5,000	1.6787	282,500
			Failure	283,300

Specimen #8A Dia. 0.8897 Area 0.6217 Material 4340 St.

Initial Stress	R-ratio	Initial Loads
42 KSI	0.1	26,111 14,361 2,611

Insp.	Max. Load	Cycles	Crack Length	Total Cycles
1	26,111	80,000	0.0560	80,000
2	26,111	20,000	0.0889	100,000
3	26,111	20,000	0.1110	120,000
4	26,111	20,000	0.1407	140,000
5	26,111	20,000	0.1984	160,000
6	26,111	20,000	0.2221	180,000
7	26,111	20,000	0.3253	200,000
8	26,111	10,000	0.3593	210,000
9	26,111	10,000	0.4840	220,000
10	26,111	10,700	0.5354	230,700
11	26,111	7,300	0.6036	238,000
12	26,111	5,000	0.6821	243,000
13	26,111	5,000	0.7647	248,000
14	26,111	5,000	0.8320	253,000
15	26,111	5,000	0.9542	258,000
16	26,111	2,500	1.0304	260,500
17	26,111	2,500	1.1168	263,000
18	26,111	2,000	1.2978	265,000
19	26,111	2,000	1.4363	267,000
20	26,111	2,000	1.6498	269,000
	26,111	1,000	failure	270,000

Specimen #9A Dia. 0.8911 Area 0.6235 Material 4340 St.

Initial Stress	R-ratio	Initial Loads
42 KSI	0.1	26,187 14,403 2,619

Insp.	Max. Load	Cycles	Crack Length	Total Cycles
1	26,187	50,000	0.0716	50,000
2	26,187	20,000	0.1043	70,000
3	26,187	20,000	0.1330	90,000
4	26,187	20,000	0.1663	110,000
5	26,187	20,000	0.2355	130,000
6	26,187	15,000	0.2976	145,000
7	26,187	15,000	0.3638	160,000
8	26,187	10,000	0.4241	170,000
9	26,187	10,000	0.4808	180,000
10	26,187	10,000	0.5308	190,000
11	26,187	10,000	0.6149	200,000
12	26,187	10,000	0.8291	210,000
13	26,187	5,000	0.8910	215,000
14	26,187	5,000	1.0673	220,000
15	26,187	2,500	1.1976	222,500
16	26,187	2,500	1.5851	227,500
		900	failure	228,400

Specimen #10A Dia. 0.8867 Area 0.6175 Material 4340 St.

Initial Stress	R-ratio	Initial Loads
38 KSI	0.1	23,465 12,906 2,347

Insp.	Max. Load	Cycles	Crack Length	Total Cycles
1	23,465	112,200	0.0753	112,200
2	23,465	20,000	0.0976	132,200
3	23,465	27,800	0.1341	160,000
4	23,465	20,000	0.1777	180,000
5	23,465	20,000	0.2321	200,000
6	23,465	20,000	0.2846	220,000
7	23,465	20,000	0.3654	240,000
8	23,465	20,000	0.4925	260,000
9	23,465	15,000	0.6168	275,000
10	23,465	10,000	0.7235	285,000
11	23,465	5,000	0.7339	290,000
12	23,465	5,000	0.8267	295,000
13	23,465	5,000	0.9182	300,000
14	23,465	5,000	1.0382	305,000
15	23,465	5,000	1.1976	310,000
16	23,465	2,500	1.3404	312,500
17	23,465	2,500	1.5226	315,000
			failure	316,700

*U.S.Government Printing Office: 1988 548-054/80793